**Atmospheric
Chemistry
and Physics
Discussions**

Seven years of measurements of aerosol scattering properties, near the surface, in the southwestern Iberia Peninsula

S. N. Pereira[1]**, F. Wagner**[1]**, and A. M. Silva**[1,2]

[1]Évora Geophysics Centre, Évora, Portugal
[2]Physics Department of the University of Évora, Évora, Portugal

Correspondence to: S. N. Pereira (sergiopereira@uevora.pt)

Discussion Paper | Discussion Paper | Discussion Paper | Discussion Paper

ACPD

10, 13723–13754, 2010

Seven years of measurements of aerosol scattering properties

S. N. Pereira et al.

Title Page

Abstract	Introduction
Conclusions	References
Tables	Figures

◄◄ ►►

◄ ►

Back Close

Full Screen / Esc

Printer-friendly Version

Interactive Discussion

Abstract

Aerosol scattering properties, near the surface, were measured over a period of seven years (2002–2008) at Évora, Portugal. This long time series provides valuable information on light scattering by aerosols, namely related with their climatology and with their direct effect on climate. The average (and median) scattering coefficient, at the wavelength of 550 nm, and the scattering Ångström exponent were found to be 42.5 Mm^{-1} (29.9 Mm^{-1}) and 1.4 (1.5) respectively, indicating that scattering is, in general, of moderate magnitude and dominated by fine particles. Both seasonal and daily cycles were shown, which were related to local production as well as with transport of particles from elsewhere. The average summer and winter values of the scattering coefficient (47 and 54 Mm^{-1} respectively), at the wavelength of 550 nm, correspond to a significant increase in the aerosol particle concentration when compared with spring and fall (35 and 37 Mm^{-1} respectively); also the simultaneous increase of the Ångström exponent, from 1.2–1.4 towards 1.4–1.6, is consistent with the input of fine particles from anthropogenic origin in winter and forest fires in summer.

Back-trajectory analysis indicate that the site was regularly under the influence of clean air masses from Atlantic area, with low particle loads (low scattering coefficients) but as the influence of transport from the continent (Iberia Peninsula) increased, the aerosol particle load was observed to increase as well as the relative importance of fine particles over coarse ones, approaching the features observed during European air masses influence.

1 Introduction

The assessment of aerosols direct effect on climate (due to their interaction with solar and terrestrial radiation, via scattering and absorption processes) requires quantitative information on the optical properties of atmospheric aerosols. The multiplicity of aerosol sources, transformation processes and sinks is responsible for the large vari-

ability in their properties both in space and time; this means that in a certain time the global aerosol concentration field is complex and at a certain place aerosol properties may also be highly variable in time. Under these circumstances long term measurements of aerosol properties at different locations are essential for better characterizing both the aerosol field and climatology, providing aerosol data to be included into global climate models in order to decrease the uncertainties of climate forcing estimations.

Previous studies on aerosol properties, at the surface (and in the column), based on measurements carried out on this region had shown that the aerosol load could be considered in general as moderate to low. Moreover the influence of long range transported aerosols from forest fires in summer and of desert dust from Sahara region (mainly at high altitudes) or the influence of anthropogenic pollution from Europe and Iberian Peninsula itself could also be clearly detected. However these studies where mainly incident on short periods; during ACE-2 (June–July 1997) and CAPEX and DARPO (May–June 2006) campaigns (Carrico et al., 2000; Müller et al., 2002; Silva et at., 2002, 2003; Ansmann et al., 2002; Wagner et al., 2009); summer periods (Elias et al., 2006); one year period (Pereira et al., 2008). For the first time a long term dataset of surface in-situ measurements of the aerosol scattering properties is used to generate aerosol climatology for a continental rural region of southwestern Europe. The multi-spectral measurements of scattering coefficients provided by a nephelometer are useful for quantifying the aerosol load and also for a qualitative distinction of aerosol events, namely those dominated by accumulation mode particles or coarse mode particles.

The multi-spectral measurements of scattering coefficients are obtained with a three wavelength Integrating nephelometer operating at Évora, Portugal, since 2002. Its measurements, during the subsequent seven years, were examined; overall statistical analysis was performed and the temporal evolution of the aerosol optical properties in different timescales (from daily to seasonal periods) was assessed.

The study is organized as follows: the sampling site and methodology are described in Sect. 2. The results and their correspondent discussions are developed in Sect. 3

and the conclusions are presented in Sect. 4.

2 Measurements and methodology

2.1 Site description

Évora (38.5° N, 7.9° W, 300 m a.s.l., ~60 000 inhabitants) is a small Portuguese city
located in the southwestern part of the Iberian Peninsula. The distance both to the
Atlantic coast and to the main populated and industrial area of great Lisbon is more
than 100 km. There are no polluting industries in the region; therefore the local an-
thropogenic sources are mainly related with traffic and wood burning during the winter
colder period; occasionally it may suffer the influence of the long range transport of
anthropogenic aerosols from major industrial or from the Saharan desert.

2.2 Equipment and dataset

A three wavelength Integrating Nephelometer (TSI-3563, TSI Inc., St. Paul, Minnesota,
USA) measured the aerosol scattering coefficients, $\sigma_{sp}(\lambda)$, and backscattering coeffi-
cients, $\sigma_{bsp}(\lambda)$, at the wavelengths λ=450, 550 and 700 nm, every 5 min. The detection
limits for total scattering coefficients are 0.44, 0.17, and 0.26 Mm^{-1} for 450, 550, and
700 nm, respectively (Anderson et al., 1996). For backscattering coefficients, the de-
tection limits are 0.29, 0.11, and 0.21 Mm^{-1} for 450, 550, and 700 nm, respectively.
The aerosol was sampled through a PM$_{10}$ sampling head located at about 10 m above
the ground, selecting particles smaller than 10 µm aerodynamic diameter. The flow
rate was fixed at 30 l min^{-1}. The scattered light in the angular range of 7–170° was
measured and the aerosol scattering coefficient was derived after correction by the
calculated molecular scattering and for the angular truncation and the non-Lambertian
errors (Anderson and Ogren, 1998); the light scattered from 90–170° (backscattered
signal) was also measured and the aerosol backscattering coefficient σ_{bsp} was also

S. N. Pereira et al.

Title Page

Abstract	Introduction
Conclusions	References
Tables	Figures

|◄ | ►|

◄ | ►

Back | Close

Full Screen / Esc

Printer-friendly Version

Interactive Discussion

derived. The instrument was calibrated at least once a year using CO_2 as high span gas and filtered dry air as low span gas; zero signal was measured once an hour.

The Ångström exponent, α, which represents the wavelength dependence of $\sigma_{sp}(\lambda)$ and can be related to a mean size of the particles, was calculated using the 450 and 700 nm channels as follows:

$$\alpha = -\frac{\log(\sigma_{sp}(700)) - \log(\sigma_{sp}(450))}{\log(700) - \log(450)} \tag{1}$$

Daily back-trajectories ending at Évora monitoring site, at 500 m a.s.l. ($\sim$200 m a.g.l.), were calculated using the Hybrid Single-Particle Lagrangian Integrated Trajectory Model (HYSPLIT) (Draxler and Rolph, 2003) to interpret data in terms of the aerosol origins; the altitude was selected to represent the air sampled by the Nephelometer. Usual meteorological data (temperature, relative humidity and wind speed and direction) was also measured at the site. Hourly averaged data (about 47 000 measurements – about 80% of overall measurements from April 2002 to December 2008) were used and longer term statistics were based on these hourly values.

Relative humidity correction

Relative humidity (RH) is one of the factors that influence the amount of scattered solar radiation by aerosol particles (Horvath, 1996). If RH increases, then non-hydrophobic atmospheric particles tend to grow due to water uptake therefore scattering more light. The factor quantifying the influence of RH on $\sigma_{sp}(\lambda)$ is the light scattering humidification factor $f(\text{RH})$ which is the ratio between $\sigma_{sp}(\lambda)$ at high RH values and at low RH values where the low RH value is considered to be lower than 40% (Kotchenruther et al., 1999; Koloutsou-Vakakis et al., 2001; Maggi and Hobbs, 2003; Targino et al., 2005).

$$f(\text{RH}) = \frac{\sigma_{sp}(\lambda)_{\text{high RH}}}{\sigma_{sp}(\lambda)_{\text{low RH}}} \tag{2}$$

In order to assess the temporal variation of the scattering coefficients, the influence of RH on $\sigma_{sp}(\lambda)$ variations has to be eliminated.

Figure 1 shows the relative frequency distributions of measured ambient RH values at the monitoring site and measured RH values inside the nephelometer's optical chamber. The difference of the two measured RH values is clear: the lower and less variable RH values measured inside the nephelometer are due to the heating produced by the lamp in the measuring sensing chamber, whereas the ambient RH values comprise a large range of values. The RH values of the sampled aerosol are constrained mainly in the range of 30–50%, centered at 40% (mean) with a standard deviation (SD) of 10%; the measurements of $\sigma_{sp}(\lambda)$ are assumed to be performed essentially with the aerosol under dry conditions and the RH corrections are expected to have minor influence in the overall results that follow in next sections. Due to the lack of measured $f(RH)$ for the sampling site, functions from the literature, corresponding to different aerosol types, were used. Errors introduced by using literature based $f(RH)$ functions are supposed to be lower than ignoring the RH dependency. The prevailing aerosol population at the site is of continental type. Anthropogenic aerosols from local or long distant sources as well as smoke aerosols from forest fires and desert dust from Africa were also present. The $f(RH)$ functions were chosen according to these aerosol types; we then distinguish between measurements made under clean/background continental conditions (the most common situation) and under perturbed conditions. The separation between different aerosol types was done by using thresholds based on absolute values of the spectral scattering coefficients and of the Ångström exponent; a previous classification scheme by Elias et al. (2006) was based only in a summer period of measurements and half day averages were considered (instead of hourly), therefore an improved classification criteria was used; these values are provided in Table 1. The correction functions for clean/background conditions were based on (Maggi and Hobbs, 2003). The correction functions for pollution data were based on (Carrico et al., 2000) whose results regard to "a continental site influenced by aerosol with anthropogenic origin". They are very similar to the ones obtained by (Koloutsou-Vakakis et al., 2001) for polluted aerosol

and (Maggi and Hobbs, 2003) for biomass burning plumes. Desert dust aerosols were assumed as being hydrophobic (Carrico et al., 2003; Fierz-Schmidhauser et al., 2009); therefore no correction for RH was applied when it dominated the aerosol population.

3 Results and discussion

3.1 General features

Here we present some basic statistics concerning the whole 2002–2008 period in order to characterize the aerosol optical properties in the region under study. Figure 2 shows the relative frequency distributions of $\sigma_{sp}(550)$ and of α hourly values derived from the nephelometer's measurements. The frequency distributions are characterized by long right tails for $\sigma_{sp}(\lambda)$ and $\sigma_{bsp}(\lambda)$ (the latter not shown) while α is left skewed. It has been shown previously (Deacon et al.,1997; Artiñano et al., 2001; Gerasopoulos et al., 2003; Freitas, 2006; Pereira et al., 2008) that the frequency distribution of scattering coefficients (or other aerosol extensive properties) can be well described by a log-normal distribution. Therefore, median values illustrate better the average conditions than the mean by decreasing the contribution of the most extreme events; this is also true for describing the average conditions of the Ångstrom exponent, α, whose frequency distribution is also skewed. The median, mean, standard deviation, 5% percentile, P5, and 95% percentile, P95, are all presented in Table 2. Log-normal parameters (modal value and geometrical standard deviation, GSD) derived for $\sigma_{sp}(\lambda)$ and $\sigma_{bsp}(\lambda)$ distributions are also shown in Table 2.

Hourly values of $\sigma_{sp}(\lambda)$ were found to be highly variable, ranging from values close to the detection limit ($\sim$0.2 Mm^{-1} for $\sigma_{sp}(550)$) up to a few extreme measurements of about 2000 Mm^{-1} recorded during forest fire plumes in August 2005 (not shown in Fig. 2 for better resolution). They mainly cover two orders of magnitude, with 98% of the values in the range of 8–250 Mm^{-1}, but most of this percentage is below 60 Mm^{-1} ($\sim$80%). The median and mean values of $\sigma_{sp}(550)$ are respectively 30 and 42 Mm^{-1} for

the whole period. The median and mean values of the Ångström exponent, 1.5 and 1.4 respectively, imply that the scattering is, in general, dominated by submicron particles (more than 80% of α values are higher than 1.0).

These results are now briefly compared with other long term measurements from other sites in the southern European region. Lyamany et al. (2009) reported average values of $\sigma_{sp}(550)=60\,\mathrm{Mm}^{-1}$ and $\alpha=1.5$ (at Granada) and Saha et al. (2008) reported a similar value of the scattering coefficient ($\sigma_{sp}(525)=60\,\mathrm{Mm}^{-1}$) (at Toulon) in larger and more populated cities in southern Spain and France, respectively. Measurements in northern Greece ($\sigma_{sp}(550)=65\,\mathrm{Mm}^{-1}$ and $\alpha=1.5$) and Israel ($\sigma_{sp}(545)=60\,\mathrm{Mm}^{-1}$) also show comparable values (Gerasopoulos et al., 2003; Derimian et al., 2006) and (Andreae et al., 2002) obtained average (and median) $\sigma_{sp}(550)=87$ (75) Mm^{-1} and $\alpha=1.4$ (1.5) at a remote site in the Negev desert. Nevertheless Vrekoussis et al. (2005) reported lower values in remote areas of Greece ($50\,\mathrm{Mm}^{-1}$) and Turkey ($45\,\mathrm{Mm}^{-1}$) and Molnár and Mészáros (2001) reported $60\,\mathrm{Mm}^{-1}$ in Hungary. These areas were observed to be influenced by local or transported continental pollution (besides desert dust) and present significantly higher average values of the scattering coefficient when compared with the ones obtained for Évora and presented in this work. As already stated above, Évora is, on the one hand, a small city with low to moderate aerosol anthropogenic influence and, on the other hand, being located in the southwestern European sector, is under the regular influence of Atlantic clean air masses, which contribute to lower aerosol concentrations levels, as already previously observed (Pereira et al., 2008; Lyamani et al., 2010).

3.2 Temporal variations

3.2.1 Annual cycle

Median and mean monthly values of $\sigma_{sp}(550)$ and α for the period of 2002–2008 are shown in the time series of Fig. 3. Figure 4 contains the yearly cycle of the same quan-

tities as a function of both the month and season considering all the measurements for each month or season (as defined in Table 3), respectively. Statistical information is summarized in Tables 3a and 3b, respectively for $\sigma_{sp}(550)$ and α. Hourly values were always used in the calculations of all statistical parameters. Regarding Fig. 3, the monthly median values of $\sigma_{sp}(550)$ range from 19 to 73 Mm^{-1} (mean values range from 23 to 92 Mm^{-1}), with only less than one quarter of these values (16 in 71 months) being higher than 40 Mm^{-1}; 14 of these 16 $\sigma_{sp}(550)$ monthly values were recorded during winter and summer periods, although the highest ones (70–73 Mm^{-1}) where recorded during the colder season. Monthly median values of α vary between 1.0 and 2.0. Moreover, the corresponding monthly median values for the 16 months referred above are the highest, ranging between 1.5 and 2.0 (3 exceptions). In contrast, the set of months with the lower monthly median values of $\sigma_{sp}(550)$, say below 25 Mm^{-1}, are within spring, autumn (and summer) periods, with the corresponding monthly median values of α having a tendency to be lower, ranging between 1.0 and 1.5.

The facts described above are in agreement with the pattern exhibited by the yearly cycles shown in Fig. 4. $\sigma_{sp}(550)$ displays a bimodal pattern with peaks in winter and summer (Fig. 4a and b) with the one from the winter being more prominent. The winter maximum is achieved in January for both the median and mean value (50 Mm^{-1} and 64 Mm^{-1} respectively); in summer the median is higher in June (34 Mm^{-1}) while the mean has its maximum in August (56 Mm^{-1}). At a large extent this is caused by occasional increases in the aerosol load due to the forest fires. The Ångström exponent, exhibited in Fig. 4c and d, follows a rather similar behavior and a reasonable positive correlation between monthly median $\sigma_{sp}(550)$ and α was found ($R^2=0.52$) as shown in Fig. 5. However, no correlation was found for the hourly values likely because for small timescales the variability of these two quantities of different nature dominates, even if at larger timescales an overall tendency is revealed. The maximum value of the monthly median α is also found in January (1.8) and a second one in both July and August (1.5). This means that globally the increase in the aerosol load is basically associated with the enhancement of particles in the sub micrometer range, either from anthro-

pogenic origin or forest fires smoke occurring in the summer season. The increase of $\sigma_{sp}(550)$ in the winter period should result from a combination of local traffic and increased emissions from heating sources (mainly wood burning) and pollution transported to the site. All these reasons are amplified by a low boundary layer thickness due to the lower atmospheric temperatures at the surface during winter, thus reducing atmospheric convection and, in consequence, pollutant dilution. In summer, forest fires are greatly responsible for the large input of particles detected at the site (Elias et al., 2006; Pereira et al., 2008) and account for major increase in the aerosol scattering coefficients. The most intense smoke plumes were observed in August 2003 and particularly in August 2005 when hourly values of $\sigma_{sp}(550)$ as high as $2000\,\mathrm{Mm}^{-1}$ were measured. These two years were, by far, the ones with the largest burnt areas ever recorded in Portugal (Autoridade Florestal Nacional, 2009). These facts are reflected in the mean $\sigma_{sp}(550)$ peak value observed in August which appears in Fig. 4a. The strong decrease in the number of forest fires in 2007 and 2008 summers is perceptible in the $\sigma_{sp}(550)$ values of Fig. 3a, as no significant peaks are visible in these periods; this led, for example, to a large difference in the monthly average and median values of $\sigma_{sp}(550)$ between August 2005 (respectively $92\,\mathrm{Mm}^{-1}$ and $39\,\mathrm{Mm}^{-1}$) and August 2008 (respectively $25\,\mathrm{Mm}^{-1}$ and $21\,\mathrm{Mm}^{-1}$); it is worth to notice that as aforementioned six of the lowest monthly median values of $\sigma_{sp}(550)$ were recorded during summer months; five of which being in 2007 and 2008 summers.

Also, the difference in the Ångström exponent between the winter and summer months is substantial, with monthly medians being in the range of 1.5–1.8 and 1.4–1.5 respectively; this is expected to be related with the dryness of the soils and well developed convection in the boundary layer during summer season which enhances the presence of coarse soil material in the atmosphere. In contrast, during winter (typical rainy season) the relative amount of coarse material is expected to be much lower, while the introduction of sub micrometer particles from wood combustion in the atmosphere in winter is more regular than the transient transport of smoke to Évora. Lyamani et al. (2008, 2010) and Saha et al. (2008) also reported annual cycles char-

Seven years of measurements of aerosol scattering properties

S. N. Pereira et al.

acterized by higher values of scattering coefficient in winter but with magnitudes significantly higher than ours (average $\sigma_{sp}(550)$=84–90 Mm^{-1} and α=1.8 and average $\sigma_{sp}(550)$>90 Mm^{-1}, respectively). In spite of the large difference in terms of aerosol concentration between Évora and Granada (and Toulon), in winter, the difference between the values of α are less important likely due to similarities in the origin of aerosol particles.

3.2.2 Daily cycle

Daily patterns of $\sigma_{sp}(550)$ and α values are analyzed in this section (see Fig. 6a–d). Median values instead of average values are used in order to minimize external influences and extreme events, so local aerosol features can emerge. We focus on winter and spring periods because they showed rather distinct statistical properties, as it was exposed in Sect. 3.2.1, and may be somewhat representative of colder and less colder (warmer) periods. Summer period was not considered since it was already revealed to be frequently contaminated by (at least) forest fires smoke plumes transported from other regions; furthermore distinction is made between the daily variations during week days (Monday to Friday, normal working days), and Sunday (non working day when anthropogenic activities are significantly reduced).

A daily pattern was found for $\sigma_{sp}(550)$, with morning and one late afternoon peaks, regarding the week days. This behavior is characteristic of urban areas (Lyamani et al., 2008; Andreae et al., 2008). The P25 and P75 curves also displayed in Fig. 6 show the same features and indicate consistency of this pattern regardless the day-to-day variability. The morning peak (Fig. 6a and c) is closely related to enhanced traffic activity during morning rush hour and therefore is not observed on Sundays (Fig. 6b and d) when typically the city is less active, during morning time. The boundary layer development along the day, together with the increase in convection provides conditions for particle dilution within a larger volume of air. This results in the decrease of $\sigma_{sp}(550)$ at the surface during the afternoon and a minimum around 15:00 is observed. In the

Seven years of measurements of aerosol scattering properties

S. N. Pereira et al.

late afternoon the combination of increased anthropogenic activity, due to traffic, and decrease of the boundary layer thickness lead again to the increase in $\sigma_{sp}(550)$.

The general features described above also show significant seasonal differences. Important differences between colder and warmer periods are related with boundary layer dynamics and additional anthropogenic activity associated with wood burning for heating purposes, besides the usual particle production by traffic activity along the year. These differences are visible in the patterns observed in Fig. 6a and c. In spring, both morning and late afternoon peaks of $\sigma_{sp}(550)$ values have similar magnitudes (about $32\,\mathrm{Mm}^{-1}$); however, in winter the morning peak is not only considerably higher ($39\,\mathrm{Mm}^{-1}$) than in spring but also a large difference for the late afternoon peak is now visible. The magnitude of this second peak ($64\,\mathrm{Mm}^{-1}$) represents a twofold increase relative to spring conditions, and emphasizes the importance of wood burning, which typically begins in the late afternoon and is likely the reason for the difference (by a factor of 1.6) to the morning peak in winter.

In spite of higher $\sigma_{sp}(550)$ values in winter, at all times, two periods of the day with minimum values (early morning, 05:00–06:00 and middle afternoon, around 15:00) present the lowest differences in $\sigma_{sp}(550)$ between winter and spring ($<3\,\mathrm{Mm}^{-1}$). Moreover, the global minimum is achieved always in the middle afternoon. On the one hand, in both of these periods the source activities are reduced while the particle removal processes are always active; on the other hand, the dilution of particles is enhanced in the developed boundary layer which occurs in the afternoon, after the solar heating of the surface. Both these features contribute to the decrease in the particle load, independently of the season, and probably explain the similarity of $\sigma_{sp}(550)$ values in these time hours of the day.

The daily variation of the Ångström exponent can be assessed by means of scatter plots relating median values of $\sigma_{sp}(550)$ with their respective values of α as shown in Fig. 7a and b. Two main differences are revealed: firstly, the magnitude of α (1.1–1.4) in spring is lower than in winter (1.5–1.9); secondly, in winter the correlation between $\sigma_{sp}(550)$ and α appears to be consistent validating the connection between the aerosol

Seven years of measurements of aerosol scattering properties

S. N. Pereira et al.

Back | Close

Full Screen / Esc

load and its anthropogenic production. In contrast, during spring the values of α reveal no particular trend (as suggested by the lack of correlation between $\sigma_{sp}(550)$ and α).

3.3 Influence of air mass history on the aerosol properties

Airborne particles detected at a certain site may have been produced locally or trans-
ported from elsewhere. In this section the measured aerosol optical properties are associated with back trajectories paths in order to infer, in a simple way, on the influence of the emission sources upon the aerosol load and type over Évora, at the surface. Daily back trajectories arriving at the monitoring site, at 500 m, were computed at 12:00 UTC. In spite of their complexity and variability they were classified into five dif-
ferent types. The hourly averages (between 12:00 and 13:00) of measured quantities, $\sigma_{sp}(550)$ and α, were used. By doing so, temporal agreement between the trajectories arrival and measured aerosol optical properties is guaranteed disregarding the local aerosol production influence and enhancing the influence of long range transport. The back trajectories classification includes the influence of Europe (EU), Africa (AF) and
the Iberian Peninsula (IB) itself (re circulations within IB). As the airflow is generally from west to east the Atlantic maritime (M) influence predominates. However, as the measurement's site is located inland, we distinguish between two levels of continental influence on the maritime trajectories. About half of the trajectories from the Atlantic sector reach Évora after a significant path over the IB, either northern path or due to
re circulations within the IB. These back trajectories were classified as MIB. Figure 8 shows, in a simplified scheme, these features.

Figure 9 shows the relative frequency distributions of $\sigma_{sp}(550)$ and of α values according to the different trajectories classification while the correspondent average and median values are shown in Table 4. The difference in the respective aerosol prop-
erties seems to validate the separation between M and MIB trajectories. The values of $\sigma_{sp}(550)$ are systematically low (and narrow distributed, essentially below 40 Mm^{-1}) for M trajectories but as soon as the air masses increase their continental influence (i.e. become MIB) a large portion of $\sigma_{sp}(550)$ values increase considerably. Also the

Ångström exponent distribution is also shifted towards larger values and values <1 become much less frequent. This simultaneous enhancement both in $\sigma_{sp}(550)$ and α points up that the increase in the aerosol load is related with the input of fine particles with Iberian origin (in conjunction with the gradual deposition and loss of influence of maritime coarse particles). Also the similarity between the average/median values of α for MIB and for EU and IB trajectories (1.6–1.7) and the increase in $\sigma_{sp}(550)$ for EU and IB trajectories (from 26.5 Mm^{-1} for MIB to 32.7 and 43.1 Mm^{-1}) corroborates the previous statements; recirculation of the air masses within the Iberian related with low advection conditions induce the accumulation of pollutants and likely validates the higher values of $\sigma_{sp}(550)$ which characterize the IB regime. Concerning the African trajectories, they're also characterized by high values of $\sigma_{sp}(550)$. The frequency distribution of α includes again an important contribution of values below 1.0 (median=1.4), which is consistent with the influence of coarse dust particles; however high α values, well above 1.0, still dominate. This means that when trajectories have African origin desert dust particles usually do not dominate the aerosol at the ground or are not even present, and the higher aerosol loads could be caused mainly by anthropogenic particles. Previously Elias et al. (2006) and Derimian et al. (2006) also stated that the long-range transport of mineral dust occurred at high altitudes.

4 Conclusions

Aerosol scattering properties, near the surface, were measured over a period of seven years (2002–2008) at Évora, Portugal.

The average (and median) $\sigma_{sp}(550)$, $\sigma_{bsp}(550)$ and α were found to be 42.5 Mm^{-1} (29.9 Mm^{-1}), 5.9 Mm^{-1} (4.4 Mm^{-1}) and 1.4 (1.5) respectively, which means that the overall aerosol population is dominated by fine mode particles and the aerosol load can be considered as moderate to low.

Both seasonal and daily cycles were shown, which were related with local features

as well as transport of particles from elsewhere. The average summer and winter values of the scattering coefficient (47–54 Mm^{-1}), at the wavelength of 550 nm, represent a significant increase in the aerosol particle concentration, when compared with spring and fall (35–37 Mm^{-1}); the simulteneous increase in the Ångström exponent is
5 consistent with the input of fine particles from anthropogenic origin and forest fires in summer.

The daily variation of the scattering coefficient is related to the local anthropogenic activities, with morning and afternoon peaks, besides the boundary layer dynamics; consistently, the morning peak is nearly absent during Sundays.

10 The measured optical properties were shown to be quite dependent on the influence of different air masses present at the site. When the site under the influence of clean air masses from Atlantic low particle loads (low scattering coefficients) were observed, but as the influence of the continent (Iberia Peninsula) increased, the aerosol particle load was also observed to increase, as well as the Ångström exponent, approaching
15 the features observed during European air masses influence. During African influence, high values of the scattering coefficients were also observed, but with smaller Ångström exponent due to the contribution of dust particles; however, in general the scattering was still dominated by fine particles indicating that dust at the surface was not so frequent because it is usually transported at high altitudes.

25 **References**

Anderson, T. L. and Ogren, J. A.: Determining aerosol radiative properties using the TSI 3563 integrating Nephelometer, Aerosol Sci. Technol., 29, 57–69, 1998.

Andreae, T. W., Andreae, M. M., Ichoku, C., Maenhaut, W., Cafmeyer, J., Karniely, A., and Orlovsky, L.: Light scattering by dust and anthropogenic aerosol at a remote site in the Negev desert, Israel, J. Geophys. Res., 107(D2), 4008, doi:10.1029/2001JD900252, 2002.

Ansmann, A., Wagner, F., Müller, D., Althausen, D., Herber, A., von Hoyningen-Huene, W., and Wandinger, U.: European pollution outbreaks during ACE 2: Optical particle properties inferred from multiwavelength lidar and star-Sun photometry, J. Geophys. Res., 107(D15), 4259, doi:10.1029/2001JD001109, 2002.

Artiñano, B., Querol, X., Salvador, P., Rodríguez, S., Alonso, D. G., and Alastruey, A.: Assessment of airborne particulate levels in Spain in relation to the new EU-directive, Atmos. Environ., 35 (Suppl. 1), S43–S53, 2001.

Autoridade Florestal Nacional: Relatório – Áreas ardidas e ocorrências em 2008, online available at: http://www.afn.min-agricultura.pt/portal, 2009.

Carrico, C. M., Rood, M. J., Ogren, J. A., Neusüß, C., Wiedensohler, A., and Hintzenberg, J.: Aerosol optical properties at Sagres, Portugal, during ACE-2, Tellus B, 52, 694–715, 2000.

Carrico, C. M., Kus, P., Rood, M. J., Quinn, P. K., and Bates, T. S.: "Mixtures of pollution, dust, sea salt, and volcanic aerosol during ACE-Asia: Radiative properties as a function of relative humidity", J. Geophys. Res., 108(D23), 8650, doi:10.1029/2003JD003405, 2003.

Deacon, A. R., Derwent, R. G., Harrison, R. M., Middleton, D. R., and Moorcroft, S.: Analysis and interpretation of measurements of suspended particulate matter at urban background sites in the United Kingdom, Sci. Total Environ., 203, 17–36, 1997.

Delene, D. J. and Ogren, J. A.: Variability of aerosol optical properties at four North American surface monitoring sites, J. Atmos. Sci., 59, 1135–1150, 2002.

Derimian, Y., Karnieli, A., Kaufmann, Y. J., Andreae, M. O., Andreae, T. W., Dubovik, O., Maenhaut, W., Koren, I., and Holben, B. N.: Dust and pollution aerosols over the Negev desert, Israel: Properties, transport and radiative effect, J. Geophys. Res., 111, D05205, doi:10.1029/2005JD006549, 2006.

Draxler, R. R. and Rolph, G. D.: HYSPLIT (Hybrid Single-Particle Lagrangian Integrated Trajectory) model access via NOAA ARL READY Website, NOAA Air Resources Lab., Silver Spring, MD. online available at: http://www.arl.noaa.gov/ready/hysplit4.html, (last access: December 2009) 2003.

Elias, T., Silva, A. M., Belo, N., Pereira, S., Formenti, P., Helas, G., and Wagner, F.: Aerosol extinction in a remote continental region of the Iberian Peninsula during summer, J. Geophys. Res., 111, D14204, doi:10.1029/2005JD006610, 2006.

Freitas, C.: Synoptic and Mesoscale Meteorological Patterns During PM Events in Lisbon Area. Master thesis, University of E' vora, 189 pp., 2006.

Gerasopoulos, E., Andreae, M. O., Zerefos, C. S., Andreae, T. W., Balis, D., Formenti, P., Merlet, P., Amiridis, V., and Papastefanou, C.: Climatological aspects of aerosol optical properties in Northern Greece, Atmos. Chem. Phys., 3, 2025–2041, doi:10.5194/acp-3-2025-2003, 2003.

Horvath, H.: Spectral extinction coefficients of rural aerosol in southern Italy – a case study of cause and effect of variability of atmospheric aerosol, J. Aerosol Sci., 27(3), 437–453, 1996.

Koloutsou-Vakakis, S., Carrico, C. M., Kus, P., Rood, M. J., Li, Z., Shrestha, R., Ogren, J. A., Chow, J. C., and Watson, J. G.: Aerosol properties at a midlatitude Northern Hemisphere continental site, J. Geophys. Res., 106(D3), 3019–3032, 2001.

Kotchenruther, R. A., Hobbs, P. V., and Hegg, D. A., Humidification factors for atmospheric aerosols off the mid-Atlantic coast of the United States, J. Geophys. Res., 104(D2), 2239–2251, 1999.

Lyamani, H., Olmo, F. J., and Alados-Arboledas, L.: Light scattering and absorption properties of aerosol particles in the urban environment of Granada, Spain, Atmos. Environ., 42, 2630–2642, 2008.

Lyamani, H., Olmo, F. J., and Alados-Arboledas, L.: Physical and optical properties of aerosols over an urban location in Spain: seasonal and diurnal variability, Atmos. Chem. Phys., 10, 239–254, doi:10.5194/acp-10-239-2010, 2010.

Magi, B. I. and Hobbs, P. V.: Effects of humidity on aerosols in southern Africa during the biomass burning season, J. Geophys. Res., 108(D13), 8495, doi:10.1029/2002JD002144, 2003.

Mólnar, A. and Mészáros, E.: On the relation between the size and chemical composition of aerosol particles and their optical properties, Atmos. Environ., 35, 5053–5058, 2001.

Müller, D., Ansmann, A., Wagner, F., Franke, K., and Althausen, D.: European pollution outbreaks during ACE 2: Microphysical particle properties and single-scattering albedo inferred from multiwavelength lidar observations, J. Geophys. Res., 107(D15), 4248, doi:10.1029/2001JD001110, 2002.

Pereira, S., Wagner, F., and Silva, A. M.: Scattering properties and mass concentration of local and long range transported aerosols over the south western Iberian Peninsula, Atmos. Environ., 42, 7623–7631, 2008.

Saha, A., Mallet, M., Roger, J. C., Dubuisson, P., Piazzola, J., and Despiau, S.: One year measurements of aerosol optical properties over an urban coastal site: Effect on local direct

Seven years of measurements of aerosol scattering properties

S. N. Pereira et al.

Title Page

Abstract	Introduction
Conclusions	References
Tables	Figures

|◄ | ►|

◄ | ►

Back | Close

Full Screen / Esc

Printer-friendly Version

Interactive Discussion

radiative forcing, Atmos. Res., 90, 195–202, 2008.

Schmidhauser, R., Zieger, P., Weingartner, E., Gysel, M., DeCarlo, P. F., and Baltensperger, U.: Aerosol light scattering at high relative humidity at a high alpine site (Jungfraujoch), European Aerosol Conference 2009, Abstract T047A07, 2009.

5 Silva, A. M., Bugalho, M. L., Costa,M. J., von Hoyningen-Huene, W., Schmidt, T., Heintzenberg, J., and Henning, S.: Aerosol optical properties from columnar data during the second Aerosol Characterization Experiment on the south coast of Portugal, J. Geophys. Res., 107(D22), 4642, doi:10.1029/2002JD002196, 2002

Silva, A. M., Costa, M. J., Elias, T., Formenti, P., Belo, N., and Pereira, S.: Ground based aerosol
10 monitoring at Évora, Portugal, Global Change Newsletter, Issue No. 56, 6–9, December 2003.

Targino, A. C., Noone, K. J., Öström, E.: Airborne in situ characterization of dry aerosol optical properties in multi-source influenced marine region, Tellus, 57B(3), 247–260, 2005.

Vrekoussis, M., Liakakou, E., Kocak, M., Oikonomou, K., Sciare, J., and Mihalopoulos, N:
15 Seasonal variability of optical properties of aerosols in the eastern Mediterranean, Atmos. Environ., 39, 7083–7094, 2005.

Wagner, F., Bortoli, D., Pereira,S., Costa, M. J., Silva, A. M., Weinzierl, B., Esselborn, M., Petzold, A., Rasp, K., Heinold, B., and Tegen, I.: Properties of dust aerosol particles transported to Portugal from the Sahara desert, Tellus, 61B,(1), 297–306, 2009.

Title Page

Abstract | Introduction

Conclusions | References

Tables | Figures

◄ | ►

◄ | ►

Back | Close

Full Screen / Esc

Printer-friendly Version

Interactive Discussion

Table 1. Used criteria for different aerosol types in terms of spectral scattering coefficients and Ångström exponent.

Aerosol type	Measured optical properties
Clean/background	$\sigma_{sp}(450){<}60\,\mathrm{Mm}^{-1}$ (any α)
Pollution and Forest fires	$\sigma_{sp}(450){>}60\,\mathrm{Mm}^{-1}$ ($\alpha{>}1$)
Desert dust	$\sigma_{sp}(700){>}30\mathrm{M}\,\mathrm{m}^{-1}$ ($\alpha{<}1$)

Table 2. Basic statistical parameters of $\sigma_{sp}(\lambda)$, $\sigma_{bsp}(\lambda)$ and α for the period of 2002–2008. The latter does not have GSD because its frequency distribution is not log-normal.

Parameter	Median	Mean	SD	P5	P95	Mode	GSD
$\sigma_{sp}(450)$ (Mm^{-1})	40.5	57.5	64.1	13.1	150.1	22.2	2.2
$\sigma_{sp}(550)$ (Mm^{-1})	29.9	42.5	45.9	10.1	109.9	19.9	2.1
$\sigma_{sp}(700)$ (Mm^{-1})	21.5	29.9	30.0	7.5	75.9	11.6	2.1
$\sigma_{bsp}(450)$ (Mm^{-1})	5.4	7.0	6.9	1.9	16.6	5.5	2.0
$\sigma_{bsp}(550)$ (Mm^{-1})	4.4	5.9	5.7	1.58	13.3	2.1	1.9
$\sigma_{bsp}(700)$ (Mm^{-1})	3.7	4.8	4.7	1.3	11.1	2.0	1.9
α	1.5	1.4	0.5	0.5	2.1	1.4	–

Table 3a. Basic statistical properties of $\sigma_{sp}(550)$ organized for each month and season between 2002 and 2008.

Month	N	Season	$\sigma_{sp}(550)$ (Mm^{-1}) Median		Mean		SD		P5	P95
Dec	4440		34.4		43.9		33.3		9.9	109.0
Jan	2799	winter	49.9	40.2	64.1	53.5	52.7	46.1	13.8	163.3
Feb	2741		42.7		58.2		52.9		9.2	152.1
Mar	4191		30		39.3		31.6		10.7	94.2
Apr	4774	spring	25.3	26.1	33.8	34.7	26.5	27.1	10.1	89.9
May	5002		24.4		31.7		22.3		10.7	78.7
Jun	4763		34.4		43.7		30.5		12.1	99.7
Jul	4493	summer	32.7	32.8	43.8	47.1	38.9	66.3	10.4	111.8
Aug	3376		31.3		56.1		114.0		9.6	147.1
Sep	3391		27.5		36.9		28.7		9.4	92.7
Oct	3567	autumn	24.3	26.8	32.9	36.9	27.2	30.6	8.4	87.6
Nov	3523		28.7		40.8		34.9		9.6	109.8

S. N. Pereira et al.

Table 3b. Basic statistical properties of $\sigma_{sp}(550)$ organized for each month and season between 2002 and 2008.

Month	N	Season	Ångström exponent Median		Mean		SD		P5	P95
Dec	4440		1.8		1.6		0.5		0.7	2.2
Jan	2799	winter	1.8	1.7	1.7	1.6	0.4	0.5	1.0	2.2
Feb	2741		1.5		1.5		0.5		0.5	2.2
Mar	4191		1.3		1.2		0.5		0.3	2.0
Apr	4774	spring	1.4	1.3	1.3	1.2	0.5	0.5	0.3	1.9
May	5002		1.3		1.2		0.4		0.4	1.9
Jun	4763		1.4		1.4		0.3		0.8	1.9
Jul	4493	summer	1.5	1.5	1.4	1.4	0.4	0.4	0.7	1.9
Aug	3376		1.5		1.4		0.4		0.6	2.0
Sep	3391		1.4		1.3		0.5		0.4	2.0
Oct	3567	autumn	1.4	1.4	1.3	1.4	0.6	0.5	0.2	2.0
Nov	3523		1.5		1.5		0.5		0.6	2.1

Table 4. Average and median values of $\sigma_{sp}(550)$ and α for each trajectory type. The frequency of occurrence for each type is also shown.

Trajectory class (frequency of ocurrence)	Mean/Median $\sigma_{sp}(550)$ (Mm^{-1})	Mean/Median α
Maritime M (34%)	20.5/16.8	1.2/1.2
MaritimeIB MIB (36%)	35.4/26.5	1.6/1.6
Europe EU (21%)	40.0/32.7	1.6/1.7
Iberian IB (3%)	59.1/43.1	1.6/1.6
African AF (6%)	58.7/49.5	1.3/1.4
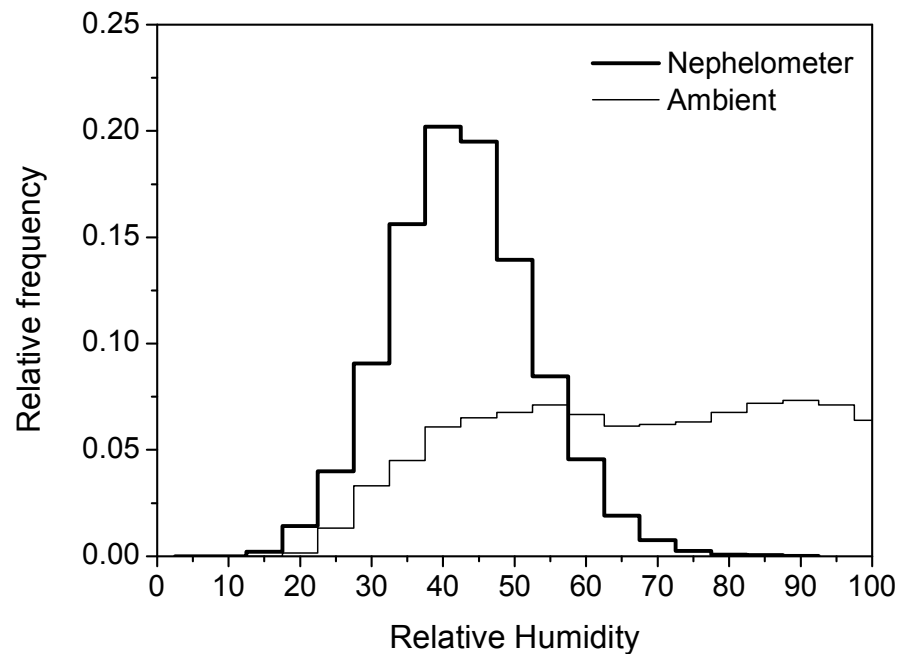
Fig. 1. Relative frequency distributions of measured ambient RH at the site and measured RH inside the nephelometer's sensing chamber.
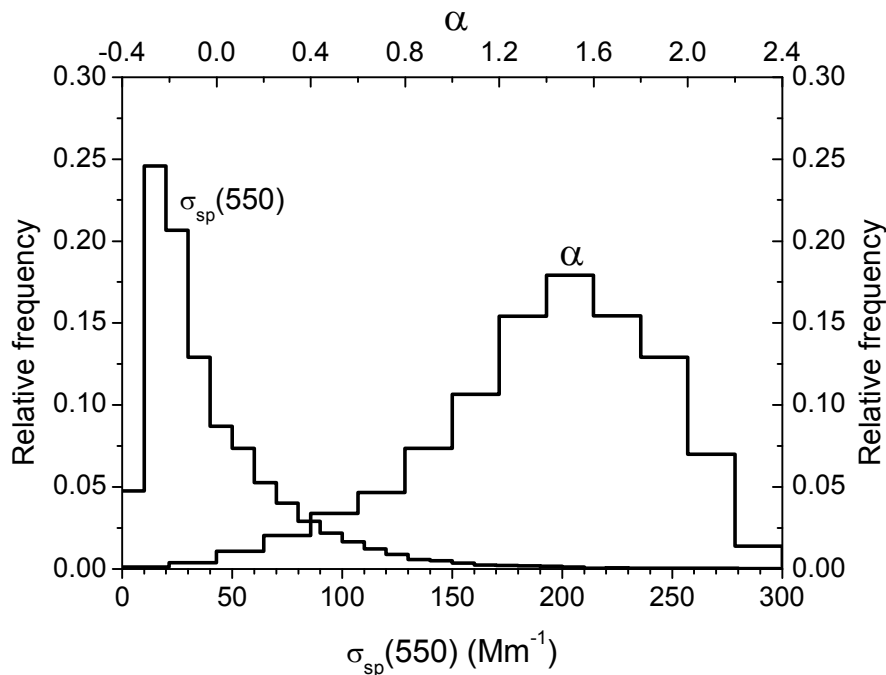
Fig. 2. Relative frequency distributions of $\sigma_{sp}(550)$ and α hourly values ($N \sim 47\,000$ and bin size of $10\,\text{Mm}^{-1}$ and 0.2 respectively). Values of $\sigma_{sp}(550) > 300\,\text{Mm}^{-1}$ (less than 100 hourly values) are not shown for better resolution.
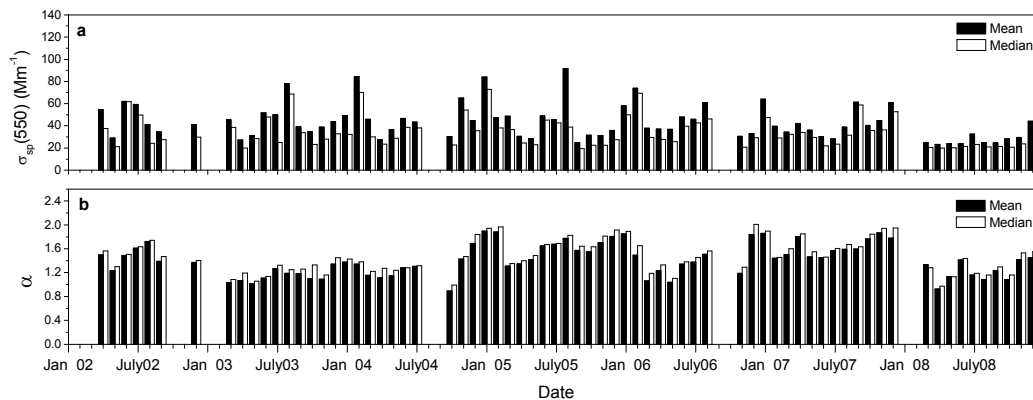
Fig. 3. Time series of mean and median monthly values of **(a)** $\sigma_{sp}(550)$ and **(b)** α.
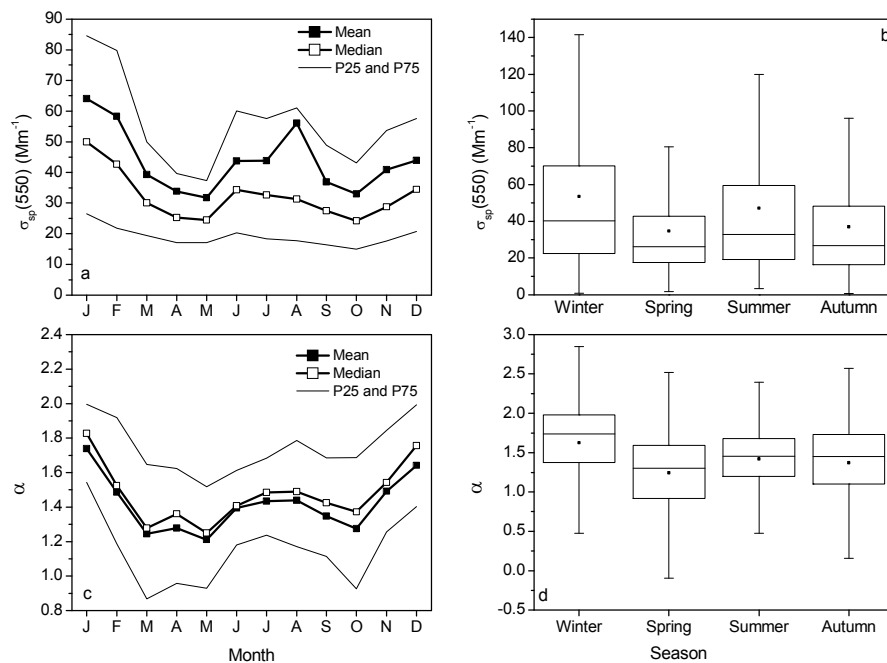
Fig. 4. Annual cycle of mean and median values of $\sigma_{sp}(550)$ (**a** and **b**) and α (**c** and **d**) as a function of the month and season. The respective quartiles (P25 and P75) are also shown. In the case of box charts P5 and P95 are also included.
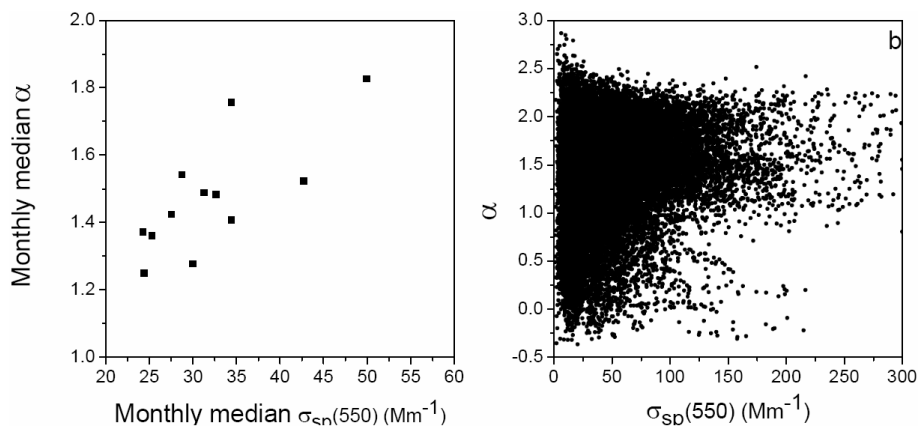
Fig. 5. Monthly median α as a function of monthly median $\sigma_{sp}(550)$ **(a)** and hourly values of the same quantities **(b)**.
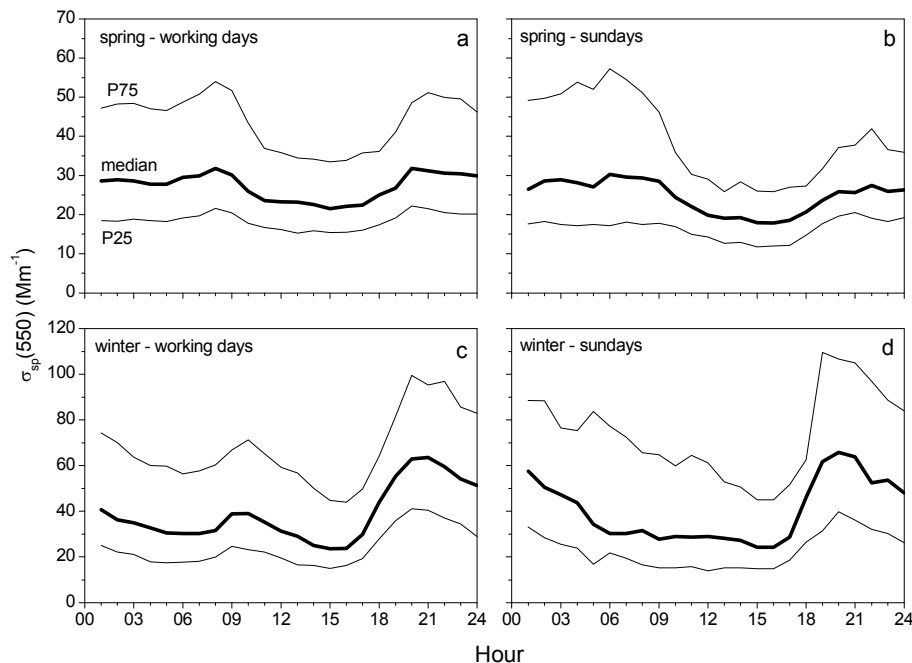
Fig. 6. Daily variation of median values of $\sigma_{sp}(550)$ for **(a)** spring working days and **(b)** Sundays and **(c)** winter working days and **(d)** Sundays. The respective quartiles are also shown.
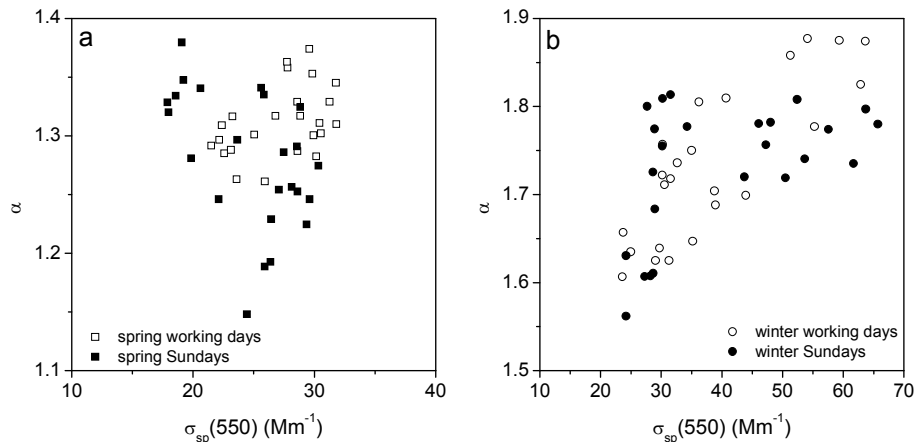
Fig. 7. Median values of α as a function of median values of $\sigma_{sp}(550)$ for spring **(a)** and winter **(b)** as well as for working days and Sundays.
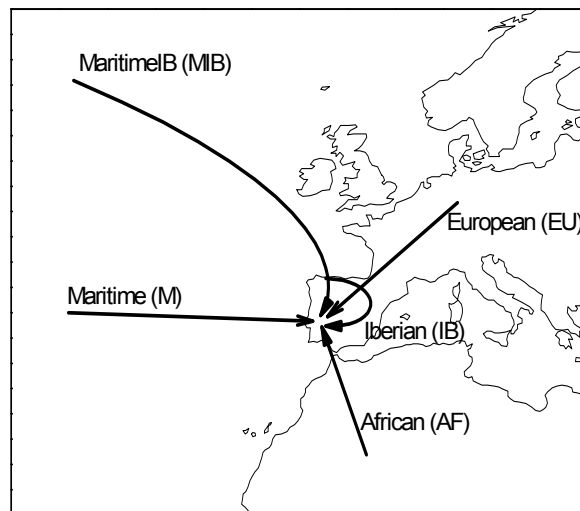
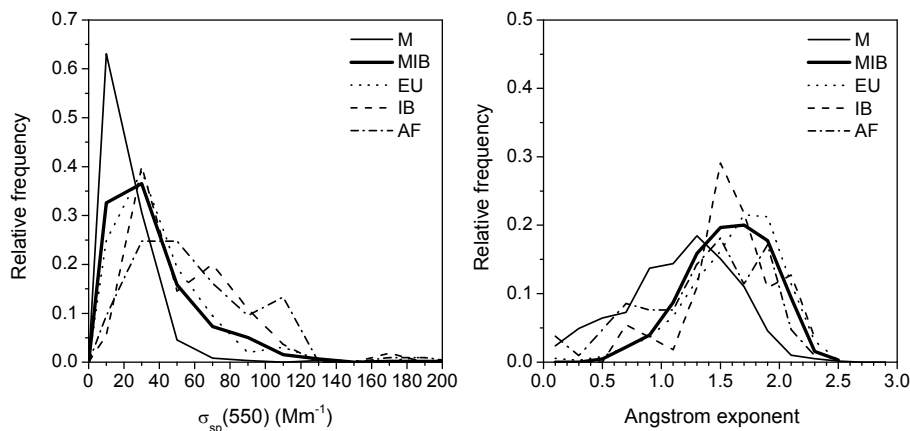**Fig. 8.** Simplified scheme with the different trajectory classes.

Fig. 9. Relative frequency distributions of $\sigma_{sp}(550)$ (bin size=20 Mm^{-1}) and α (bin size=0.2) for each trajectory type.